Modelling the hardening of gamma-ray spectra by extragalactic background light

Ayman M. Kudoda[*1]**, A. Faltenbacher**[*]

[*]School of Physics, University of the Witwatersrand, Johannesburg 2050, South Africa.

E-mail: [1]`ayman.kudoda@students.wits.ac.za`

Abstract. The interactions of Extragalactic Background Light (EBL) photons and γ-rays from distant quasars result in the steepening of the γ-ray spectrum at very high energies. The underlying process is the γ-ray absorption induced by pair production $(\gamma + \gamma' \rightarrow e^+ + e^-)$ which is dependent on γ-ray energy and EBL energy density. We present a realistic model of the EBL based on the semi-analytical galaxy catalogues from the Millennium data base plus a homogeneous component assumed to be the accumulated light from distant galaxies. This approach reflects the fluctuations in the EBL due to the inhomogeneous galaxy distribution in a realistic manner. Our model predicts well the steepening of the spectral index of distant γ-ray sources as a function of redshift. In agreement with our previous purely analytical results the differences in the opacity due to individual γ-ray paths experiencing different EBL fluctuations are negligible.

1. Introduction

The extragalactic background light (EBL) is the light integrated from all extragalactic sources since the recombination era. Consequently, it comprises a wealth of information on star formation and the evolution history of the Universe. Its spectrum lies between $0.1 - 1000\,\mu m$, with two distinct humps: a first hump between 0.1 and 10 μm due to direct stellar emission; a second hump between 10 and 1000 μm, which is caused by the dust. Measurements of the EBL can be used to provide constraints on star formation models and the baryonic matter content of the Universe [1].

Direct measurement of the EBL is difficult because of strong foreground contamination by galactic and zodiacal light. Indirect measurements have been obtained by studying the attenuation of the spectra of distance γ-ray sources. This is possible because the γ-rays emitted from distance sources (quasars) get absorbed along the way by the EBL photons through pair production $(\gamma + \gamma' \rightarrow e^+ + e^-)$. This process causes a steepening of the spectral index of the quasars in the VHE regime [2]. While the attenuation depends on the γ-ray energy and the EBL density along the line of sight. Clustering of galaxies on a scale of up to 100 Mpc causes fluctuations in the EBL density. Here we present a semi-analytical model to determine the EBL and its fluctuations based on a realistic dark matter density distribution.

Although it should be possible to constrain the EBL density and its fluctuations from observations of distant quasars, our understanding of the intrinsic source spectrum is incomplete. In fact, it is difficult to differentiate between the source-inherent effects and the signature of the EBL on the observed spectrum [3]. Figure 1 shows observed VHE spectral indices (Γs) of selected high-synchrotron-peaked BL Lac (HBL) objects as a function of redshift (data obtained from
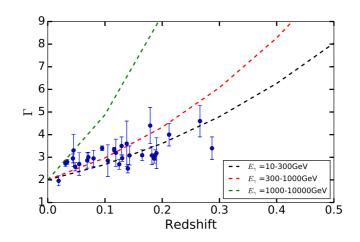
Figure 1: Observed spectral indices Γ of the hard γ-ray for HBL objects as a function of redshift (data obtained from table 1 in [4] excluding extreme HBLs and those with uncertain redshifts. The dashed lines represent the predictions of our EBL model for the observed (absorbed) Γ if the intrinsic spectrum is $\Gamma_{\text{Interact}} = 2.0$. Different lines correspond to different γ-ray energy ranges used to determine the spectral index.

table 1 in [4] excluding extreme HBLs and those with uncertain redshifts). As can be seen in the Figure, there is a clear correlation between the Γs and redshift [4]. Gamma-rays of more distant sources have a higher probability to interact with the EBL along the path and this steepen the VHE spectra.

It is interesting to find out whether the scatter in the spectral indices is an intrinsic feature of different sources or the effect of the variation in the optical depth along the path from the source to the observer. In our previous work [5, 6] (here after KF17), we developed a purely analytical framework for computing the EBL fluctuation by calculating upper and lower limits in the star formation rate (SFR) and implementing them in the EBL model by [8, 9]. Our model predicted maximum changes of $\pm 10\%$ in the γ-ray transmissivity. This is also in agreement with the result reported by [10, 11]. However, this translates into only marginal differences in the power-law slopes of the deabsorbed γ-ray spectra ($\lesssim \pm 1\%$). This variation is not enough to describe the observed scatter.

In this work we use semi-analytical galaxy catalogues from the Millennium data base [12, 13] which enable us to trace the path of the γ-ray through a more realistic EBL photon field. By generating a statistical ensemble of different γ-ray paths the stochastic distribution of γ-ray opacities can be investigated.

2. The EBL Model
In order to evaluate the EBL energy density along the γ-ray path we used the simulated MR7 galaxy catalog [12, 13] and constructed cylinders with comoving radius of 50 Mpc from $z = 0$ up to $z = 0.5$. We avoided repetition of structures along the line of sight by randomly rotating and shifting the snap-shots to match the comoving distance at a specific redshift. Figure 2 shows an example of the resulting cylinders up to $z = 0.5$. We assigned a spectrum to each galaxy in the cylinder based on its age, metallicity and mass (all properties readily extracted from MR7 catalogue) using the simple stellar populations synthesis library: bc03 [14], assuming each galaxy has single stellar populations. To get the number of photons in the stellar component we used an empirical function for the escape fraction formula [8]. Then by integrating the energy trapped by the escape fraction formula and assuming quasistatic equilibrium, the total energy trapped is

then re-radiated in the IR, distributed among three black body with temperatures (40, 70 and 450 K). We then added the stellar and the dust components to get the galaxy spectrum from ultraviolet (UV) to infrared (IR) regimes.
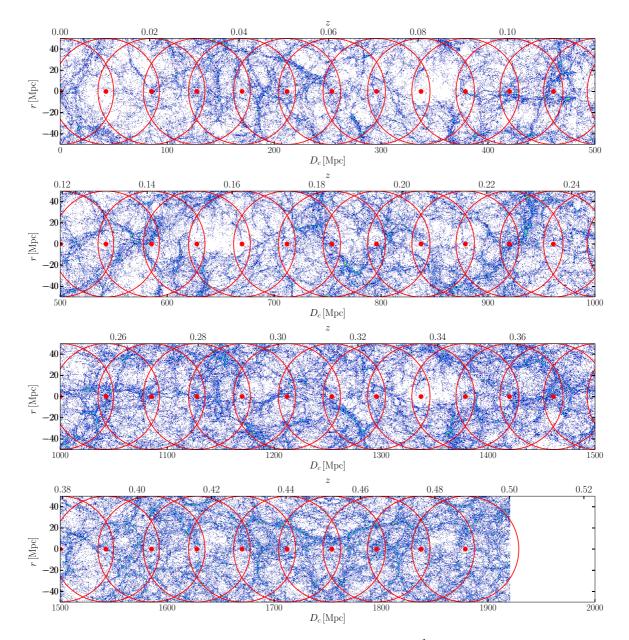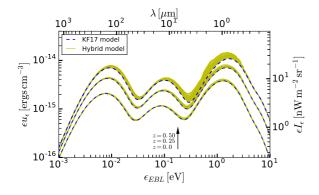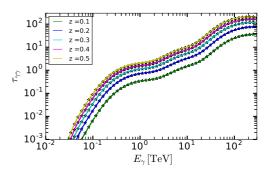

Figure 2: Light cone (cylinder) with comoving radius of 50 h^{-1}Mpc from $z = 0$ up to $z = 0.5$. The red points in the middle of the cylinder represent the locations where the local EBL density from a sphere of radius 50 Mpc (red circles) was computed.

By choosing points along the γ-ray path (central line of the cylinder) with $dz = 0.01$ separation (shown as red dots in figure 2), we computed the light contribution of the galaxies in a sphere of radius 50 h^{-1}Mpc around these points applying $1/r^2$ luminosity profile. To evaluate the total EBL energy at each z we added a homogeneous background to the local EBL density computed following [6]. Figure 3 shows the EBL spectrum at different redshifts in yellow lines with the KF17 model in blue lines. The complete model is presented in [7].

Figure 3: The EBL intensity at different redshifts in yellow lines, the blue dashed lines are the corresponding EBL intensity obtained using KF17.

Figure 4: The γ-ray opacity $(\tau_{\gamma\gamma})$ in the cylinders at different redshifts ($z = 0.1$ to $z = 0.5$) with E_γ energy range of 10^{-2} to 300 TeV in solid line, where the stars show the opacity calculated using the KF17 model.

3. Results and Discussion

With the model described above we produced a realistic EBL spectra which allow us to determine the EBL intensity along the individual γ-ray paths. Following equation No.17 in [8], we calculate the γ-ray opacity for various γ-ray paths as shown in figure 4. The figure displays the opacity at different redshifts from $z = 0.1$ up to $z = 0.5$ and γ-ray energy between $10 - 10^4$ GeV. The opacity increases rapidly above 300 GeV. This suggests different EBL attenuation effects for different γ-ray energy ranges. The opacities for the ensemble of γ-ray paths are very similar and would lie on top of each other as shown in solid lines in figure 4, and for comparison we show opacities for KF17 model in stars-lines.

Assuming $\Gamma = 2.0$ as the source's intrinsic spectral index at different redshifts, we use the opacity discussed above to compute the observed spectral index at three different energy ranges: $10 - 300$, $300 - 10^3$ and $10^3 - 10^4$ GeV, as shown in figure 1 in black, red and green dashed lines, respectively. The model spectral index retains the observed correlation with redshift. As expected, the observed spectral index steepen more rapidly if measured within increasing energy ranges.

4. Conclusion

In this paper we investigated the γ-ray opacity based on a realistic EBL model. The EBL was computed based on the simulated inhomogeneous galaxy distribution plus a homogeneous EBL component assumed to originate from galaxies at larger distances. The opacities were computed for an ensemble of γ-rays distributed throughout the simulation box. Based on the γ-ray opacity we determined the steepening of the observed spectral index of the γ-ray source with redshift. The simulated behaviour agrees with the observed steepening of the hard γ-ray spectra. The differences in the opacity due to fluctuations in the EBL (integrated EBL along various γ-ray paths) are marginal. Thus, our EBL model which, by construction, includes the contribution of individual galaxies very close to the γ-ray path cannot account for the scatter in the spectral indices seen in figure 1.

online access to them were constructed as part of the activities of the German Astrophysical Virtual Observatory (GAVO).

References

[1] Dwek E and Krennrich F 2013 *Astroparticle Physics* **43** 112
[2] H.E.S.S. Collaboration, Abramowski A, Acero F, et al. 2013 *Astronomy & Astrophysics* **5** 550 A4
[3] Mazin D and Raue M 2007 *A&A* **471** 439
[4] Sinha A, Sahayanathan S, Misra R, Godambe S and Acharya B S 2014 *ApJ* **795** 91
[5] Kudoda A M and Faltenbacher A 2015 3rd Annual Conference on High Energy Astrophysics in Southern Africa (HEASA2015) 20
[6] Kudoda A M and Faltenbacher A 2017 *MNRAS* **467** 2896
[7] Kudoda A M and Faltenbacher A 2018 *MNRAS* **481** 405
[8] Razzaque S, Dermer C D and Finke J D 2009 *ApJ* **697** 483
[9] Finke J D, Razzaque S and Dermer C D 2010 *ApJ* **712** 238
[10] Furniss A, Sutter P M, Primack J R and Domínguez A 2015 *MNRAS* **446** 2267
[11] Abdalla H and Böttcher M 2017 *ApJ* **835** 237
[12] Lemson G and the Virgo Consortium 2006 *arXiv:astro-ph/0608019*
[13] Guo Q, White S, Angulo R E, et al. 2013 *MNRAS* **428** 1351
[14] Bruzual G and Charlot S 2003 *MNRAS* **344** 1000